

Insertion of the Ca²⁺-Independent Phospholipase A₂ into a Phospholipid Bilayer via Coarse-Grained and Atomistic Molecular Dynamics Simulations

Denis Bucher^{1,2*}, Yuan-Hao Hsu³, Varnavas D. Mouchlis⁴, Edward A. Dennis^{1,4*},
J. Andrew McCammon^{1,4,5}

1 Department of Chemistry and Biochemistry, University of California, San Diego, La Jolla, California, United States of America, **2** Center for Theoretical Biological Physics and National Biomedical Computation Resource, University of California, San Diego, La Jolla, California, United States of America, **3** Department of Chemistry, Tunghai University, Taichung, Taiwan, **4** Department of Pharmacology, University of California, San Diego, La Jolla, California, United States of America, **5** Howard Hughes Medical Institute, University of California, San Diego, La Jolla, California, United States of America

Abstract

Group VI Ca²⁺-independent phospholipase A₂ (iPLA₂) is a water-soluble enzyme that is active when associated with phospholipid membranes. Despite its clear pharmaceutical relevance, no X-ray or NMR structural information is currently available for the iPLA₂ or its membrane complex. In this paper, we combine homology modeling with coarse-grained (CG) and all-atom (AA) molecular dynamics (MD) simulations to build structural models of iPLA₂ in association with a phospholipid bilayer. CG-MD simulations of the membrane insertion process were employed to provide a starting point for an atomistic description. Six AA-MD simulations were then conducted for 60 ns, starting from different initial CG structures, to refine the membrane complex. The resulting structures are shown to be consistent with each other and with deuterium exchange mass spectrometry (DXMS) experiments, suggesting that our approach is suitable for the modeling of iPLA₂ at the membrane surface. The models show that an anchoring region (residues 710–724) forms an amphipathic helix that is stabilized by the membrane. In future studies, the proposed iPLA₂ models should provide a structural basis for understanding the mechanisms of lipid extraction and drug-inhibition. In addition, the dual-resolution approach discussed here should provide the means for the future exploration of the impact of lipid diversity and sequence mutations on the activity of iPLA₂ and related enzymes.

Citation: Bucher D, Hsu Y-H, Mouchlis VD, Dennis EA, McCammon JA (2013) Insertion of the Ca²⁺-Independent Phospholipase A₂ into a Phospholipid Bilayer via Coarse-Grained and Atomistic Molecular Dynamics Simulations. *PLoS Comput Biol* 9(7): e1003156. doi:10.1371/journal.pcbi.1003156

Editor: Nir Ben-Tal, Tel Aviv University, Israel

Received: February 21, 2013; **Accepted:** June 11, 2013; **Published:** July 25, 2013

Copyright: © 2013 Bucher et al. This is an open-access article distributed under the terms of the Creative Commons Attribution License, which permits unrestricted use, distribution, and reproduction in any medium, provided the original author and source are credited.

Funding: This work was supported by NIH Grants RO1-GM20501 (EAD), and the San Diego Super computer Center (SDSC). DB and JAM were supported in part by NSF, NIH, HHMI, NBCR, and CTBP. The funders had no role in study design, data collection and analysis, decision to publish, or preparation of the manuscript.

Competing Interests: The authors have declared that no competing interests exist.

* E-mail: bucher.denis@gmail.com (DB); edennis@ucsd.edu (EAD)

Introduction

Many membrane proteins remain unexplored at the molecular-level despite their clear pharmaceutical relevance [1,2]. It is therefore crucial to develop computational methods for the structure prediction of membrane proteins. Homology modeling is a common technique to build an initial model when an appropriate template can be identified. Subsequently, all-atom (AA) molecular dynamics (MD) simulations have been used in the refinement of homology models with some success [3,4]. However, for protein-membrane systems the construction of structural models is complicated by the need to equilibrate all the possible orientations of the protein in the membrane. Because the current time-scale accessed by AA-MD (hundreds of nanoseconds) is typically too short to simulate the complete insertion process directly, an effective approach to study membrane proteins is to start with a low-resolution model and subsequently go to higher resolution. Coarse-grained (CG) models for proteins [5] such as the MARTINI force field [6,7] have been used to extend the time-scale of MD simulations by ~3–4 orders of magnitude, allowing the direct simulation of membrane insertion processes. The force field performs roughly a 4 to 1 mapping between atoms and

particles, which has been shown to be sufficiently accurate to study membrane insertion processes [8,9], including for surface enzymes [10,11]. However, like other resolution exchange methods [12,13], this approach remains relatively new and untested and structural models should be validated experimentally whenever possible.

Phospholipase A₂ (PLA₂) [1] is one of the largest protein superfamilies identified to date, with 16 groups and many subgroups resulting in more than 35 forms, and represents a promising target for computer-aided drug design (CADD) [14]. All PLA₂s stabilize at the membrane surface where they can catalyze the hydrolysis of phospholipids to yield fatty acids, involved in signaling, inflammation and in membrane maintenance [15]. The four predominant well-studied types of PLA₂s found in human tissues are the cytosolic (also known as cPLA₂), the secreted (sPLA₂), the calcium-independent (iPLA₂), and the lipoprotein-associated (Lp-PLA₂) enzymes. The structures of PLA₂s–bilayer complexes have been previously approached with deuterium exchange mass spectrometry (DXMS) [16]. These experiments provide information about the solvent accessible surface of the proteins by measuring the rate and number of backbone amide N-H groups that can exchange hydrogen with deuterium when in D₂O. In this technique, the protein is first enzymatically digested

currently no NMR or X-ray information about the iPLA₂ structure, the stability of the homology model was previously tested with MD simulations [28]. The ranking and scoring of docked compounds, as well as deuterium exchange experiments, in the presence, and in the absence of an inhibitor, also suggested that the active-site residues are well described in our model [28]. The most populated structural cluster in the AA simulations was used as the starting structure for generating the CG structural model. The same AA structure was also used for fitting atomic coordinates into equilibrated CG coordinates of the membrane complex, as described in the next subsection. All CG-MD simulations were conducted with GROMACS 4.5.4 [31]. The MARTINI 2.1 force field was used for the protein [7], together with non-polarizable CG water particles [6]. To maintain the protein secondary and tertiary structure an elastic network was applied composed of harmonic restraints (with a force constant of $10 \text{ kJ mol}^{-1} \text{ \AA}^{-2}$) between all backbone particles within 7 \AA of each other [32]. Palmitoyl oleoyl-phosphatidylcholine (POPC) molecules were used for the lipid membrane simulations, because the iPLA₂ is known to be active on this type of membrane [33]. The final simulation system was neutral and contained the protein, 390 randomly positioned POPC molecules, and 11871 CG water particles. The chosen CG water model does not bear charges, and it is blind to electrostatic fields and polarization effects. To compensate for the neglect of explicit polarization, screening of electrostatic interactions is done implicitly, assuming a uniform relative dielectric constant of 15 that is smoothly shifted to zero between 0 and 12 \AA [6]. The initial box dimensions were $140 \times 140 \times 140 \text{ \AA}^3$. Prior to the production runs, energy minimization was carried out for 5000 steps using a steepest-descent algorithm. The integration timestep in CG-MD simulations was 25 fs. Temperature was kept constant at 323 K using the velocity rescaling thermostat of Bussi *et al* [34]. A Berendsen barostat [35] was used to apply anisotropic pressure coupling, using a coupling constant of 10.0 ps, a compressibility value of $3 \times 10^{-3} \text{ bar}^{-1}$, and a reference pressure of 1 bar. Van der Waals interactions were also smoothly shifted to zero between 9 and 12 \AA [6]. For simplicity, the time-scale of CG simulations is reported here without a scaling factor; it is however possible to use a scaling factor of ~ 4 to account for the speed-up in the diffusive dynamics of the CG water model with respect to real water [7]. During the CG-MD simulations, the bilayer was found to self-assemble in the presence of the protein within $\sim 50 \text{ ns}$, leading to a local energy minimum. A total simulation time of $\sim 30 \mu\text{s}$ was accumulated to obtain ample statistics about the enzyme–membrane association process.

AA-MD simulations

The AA models were built in VMD [36] by aligning our best equilibrated AA structure onto the CG structures for the membrane complex, using a least squares fitting of alpha carbons on CG particles. Following this, an equilibrated POPC membrane patch of area $103 \times 103 \text{ \AA}^2$ was aligned on the CG membrane phosphate groups. Lipids within 0.6 \AA of the protein were removed, and the system was solvated with TIP3P water. 42 Na⁺ and Cl⁻ ions were added to create a solution with a physiological ion concentration of $\sim 0.1 \text{ mol/L}$. The AA simulations were conducted in NAMD 2.9 [37] with the CHARMM36 force field [38,39], using a time step of 2 fs in combination with the SHAKE algorithm [40]. Long-range electrostatic interactions were calculated using the particle mesh Ewald method, and van der Waals interactions utilized a cutoff of 10 \AA . The temperature was regulated with a Langevin thermostat [41], using a damping coefficient of 5 ps^{-1} . Energy-minimization was carried out for 10,000 steps, followed by an equilibration simulation in the NPT

ensemble of 10 ns. Positional restraints (force constant $10 \text{ kJ mol}^{-1} \text{ \AA}^{-2}$) were applied to the protein during equilibration, while the system was slowly heated-up, from 0 to 310 K, by 1 K every 4 ps. Water was prevented from entering the empty space between the protein and the membrane using a repulsive potential implemented in NAMD as an external Tcl script. At the end of the equilibration phase, the protein structure was released. Six AA-MD simulations were initiated from CG structures generated by extensive CG-MD sampling and separated by at least $1 \mu\text{s}$. The six simulations were conducted in the NPT ensemble with isotropic pressure scaling, and lasted for 60 ns. The coordinates of an equilibrated AA system are included as supporting information (Text S1). To analyze the structure of the iPLA₂–membrane complex, both the insertion depth and the insertion angle were monitored. We define the insertion angle as the angle between the long helix (residues 724 to 750) and its projection on the membrane surface. The depth of penetration is measured as the distances between the center-of-mass (c.o.m.) of the alpha carbons of anchor residues, and the c.o.m. of the bilayer along the bilayer normal (z axis). Finally, two additional AA-MD simulations in solution were conducted for 100 ns, in order to compare the properties of the iPLA₂ catalytic domain in solution and in the membrane.

Results

Our results are discussed in the following order: First, CG-MD simulations are reported for the protein insertion process. Second, we discuss the refinement of AA models generated from the CG structures for the membrane complex. Third, we describe residues in contact with the membrane and compare our results with H/D exchange experiments. Finally, we make some concluding comments about the mechanism of lipid extraction.

CG-MD simulations of the protein insertion process

Two different approaches were employed to study the insertion of iPLA₂ into a phospholipid bilayer with CG-MD (Figure 2). In the first approach (Figure 2A), ten CG-MD simulations of $\sim 500 \text{ ns}$ were conducted starting from a random configuration of the lipids around the protein. The membrane was found to self-assemble within $\sim 50 \text{ ns}$ into a fully formed phospholipid bilayer. In seven out of these ten simulations, the bilayer formed around the protein and the enzyme–membrane complex equilibrated with the enzyme adopting an interfacial location. In the other three simulations, the bilayer formed and the enzyme remained in the aqueous environment for the entire simulation. In the second approach (Figure 2B), the membrane was already formed and the protein was in solution, and three long CG-MD simulations were conducted. The time before the onset of anchoring was much longer in this case: $\sim 2.5 \mu\text{s}$, $3.2 \mu\text{s}$, and $4.1 \mu\text{s}$. Inspection of the trajectories reveals that multiple collisions between the enzyme and the membrane occurred before the formation of the enzyme–membrane complex. More specifically, insertion occurred only when the enzyme collided with its anchoring region (residues 710 to 724) pointing toward the membrane, and therefore, $\sim 90\%$ of the collisions between the protein and the membrane were unproductive. After adopting an interfacial location, iPLA₂ remained at the interface for the remainder of each simulation, consistent with a stable configuration. In Figure 2C, an alignment of the resulting iPLA₂–membrane structures with both approaches is shown. A limitation of the first approach is that the membrane can form too rapidly around the protein, and kinetically trap a less stable conformation that corresponds only to a local minimum. This occurred in two of the seven simulations, leading to a

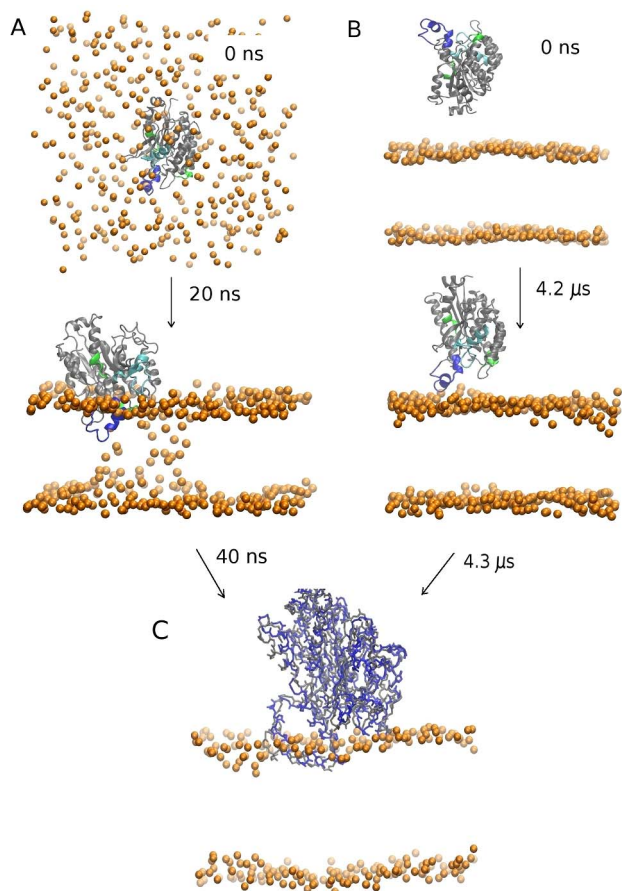


Figure 2. Snapshots from the CG-MD simulations showing the stabilization of the iPLA₂ catalytic domain at the membrane surface. In (A), the membrane self-assembly was simulated starting from a random distribution of the phospholipids around the protein; and in (B), the membrane was formed at the beginning of the simulations with the protein in solution. The protein is colored in blue for residues that are inside the membrane according to DXMS results (see next subsections), and in green and light blue for residues that display only a weak decrement in H/D exchange consistent with a position above the membrane surface. Phospholipid phosphate particles are shown in orange. (C) The resulting structures for the iPLA₂-membrane complex obtained with methods A and B are shown superimposed (backbone atoms only). doi:10.1371/journal.pcbi.1003156.g002

conformation with a lower insertion angle of ~ 10 deg. The second CG-MD approach did not appear to suffer from this limitation, but it required hundred times longer simulations to observe successful insertion events.

AA-MD refinement of the enzyme-membrane models

An important methodological question concerns the ability of multi-scale simulations to generate a unique atomistic structure for the iPLA₂-membrane complex that corresponds to the global energy minimum. To bring back an all-atoms level of details, six AA-MD simulations were seeded from distinct CG structures of the catalytic domain at the membrane surface. AA-MD simulations were conducted for 60 ns to allow the relaxation of the protein structure that was previously restricted by the use of an elastic network. Detailed interactions such as hydrogen bonding are not represented in the chosen CG model, but were probed with AA-MD. We found that in all six AA-MD simulations, the

equilibration of side-chains lead to additional hydrogen bonds with the phospholipids headgroups that equilibrated within ~ 20 ns (Figure 3C). Importantly, no significant drift occurred in AA trajectories initiated from the CG structures, and for all six simulations the protein structures could be aligned with a root-mean-square deviation (RMSD) for backbone atoms below 4 Å. In addition, the residues in contact with the lipid headgroups/tails, and the insertion angle (67 ± 8 deg), were in agreement between all simulations within the naturally occurring fluctuations (Figure 3C,D).

The stability of the AA models was further examined by MD relaxation from high-energy structures. Four new models were generated in two tense orientations on the membrane: two models were positioned perpendicularly 3 Å, and 6 Å, deeper into the membrane than the equilibrium model; the other two were tilted by +15 degree (deg), and -15 deg angles. After equilibration of the membrane for 10 ns, the protein was allowed to relax and the changes in the orientation and depth of the protein were monitored for over 40 ns. These simulations were conducted at 340 K to accelerate the protein relaxation. In all four simulations, the average displacement with respect to the initial structure was >6 Å and indicated that the protein has not yet reached a stable position after 40 ns. The simulations also showed a significant displacement of the enzyme out of the lipid bilayer when the insertion was too deep. Similarly, the tilted enzyme models rotate toward the original binding model as expected. Thus, in both relaxation experiments, the enzyme transits from a tense mode to a relaxed mode and slowly converges toward our best guess for the protein position, suggesting that it corresponds to a favorable conformation at the membrane surface. Therefore, we conclude that our multi-scale simulation approach is robust for determining the lowest energy structure for the iPLA₂-membrane complex.

Figure 3A shows a representative snapshot of an equilibrated AA-MD simulation, and highlights the membrane surface, the anchoring region, and the contours of a protein cavity at the membrane surface. In all six equilibrated structures, the same surface of the protein was found to bind to the membrane. In particular, three regions are in direct contact with the membrane (regions 552-555, 643-646, and 710-724). The main contact region (710-724, shown in Figure 3B) folds into an amphipathic alpha helical structure that is inserted into the membrane. One side of the helix consists of a cluster of hydrophobic residues (Pro711, Pro714, Trp715, Leu717, Val721, and Phe722) that have their side-chains pointing toward the lipid tails and act as hydrophobic anchors. The other side of the helix consists of basic (Arg710, and Lys719) and polar residues (Ser712, Asn713, Glu716, Thr720, and Gly723) that mainly interact with the lipid headgroups. In addition, a second region (643-646) contains Try643 and Arg645 that can also interact with the membrane surface. Tyrosine and arginine residues are known to bind near the lipid tail/headgroups interface, as they can create both favorable hydrogen bonds and hydrophobic interactions. Finally, a third contact region (552-555) helps to stabilize the angle between the protein and the membrane. It is formed by Arg553 that can interact with the lipid headgroups, Pro554 that can interact with the lipid tails, as well as Ser552 and Tyr555 that can form hydrogen bonds with the headgroups. In the CG-MD simulations, the insertion angle was about ~ 45 deg when Arg553 was unable to form a hydrogen bond with the lipid headgroups, but it equilibrated to >65 deg when this interaction was formed.

The depth of penetration of iPLA₂ into the lipid bilayer was assessed by measuring the distances between the center-of-mass (c.o.m.) of the alpha carbons relative to the c.o.m. of the bilayer,

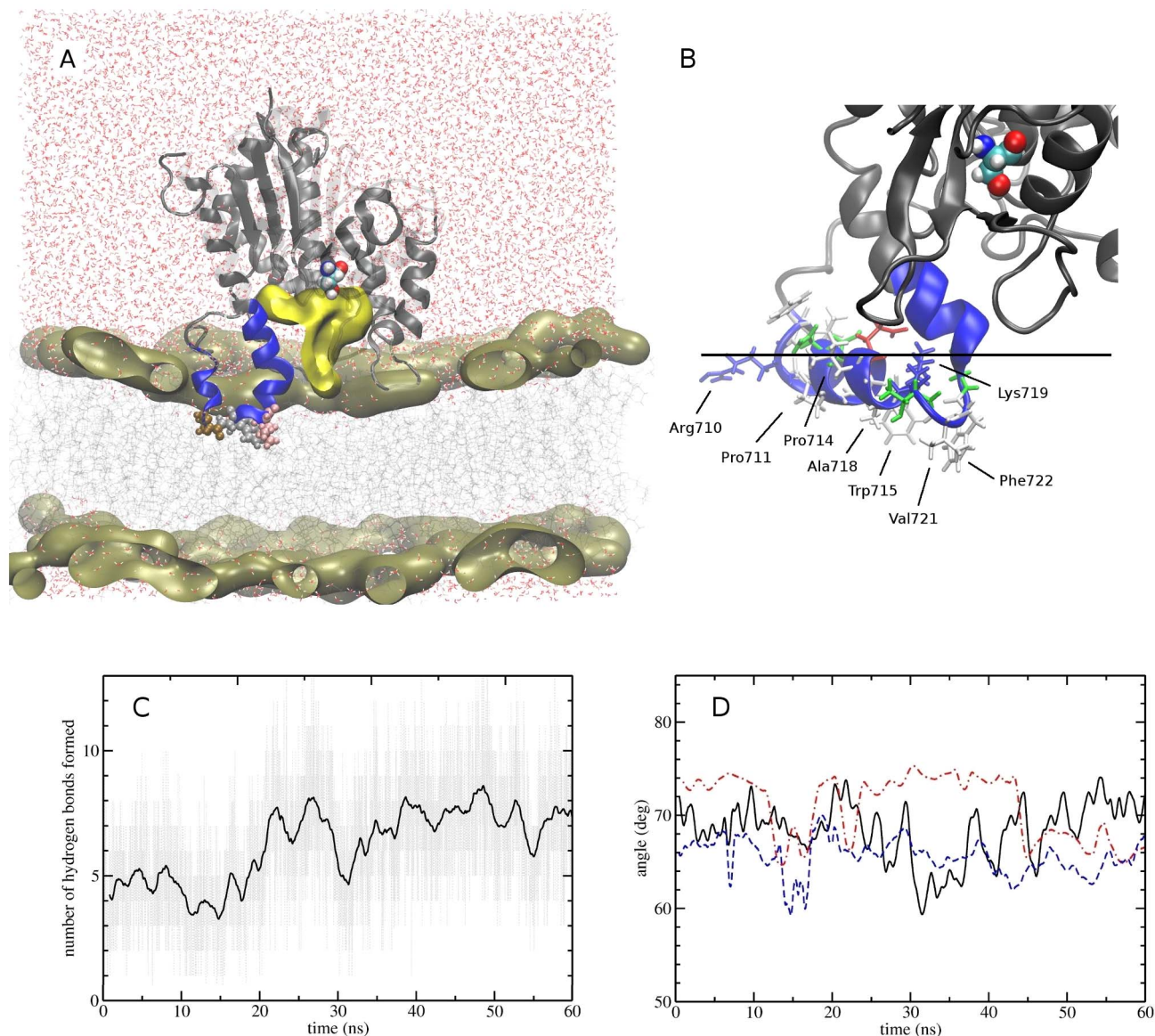


Figure 3. Atomistic MD simulation of the catalytic domain of iPLA₂ in a lipid bilayer. (A) Cutaway view of the catalytic domain inserted into the lipid bilayers from a representative snapshot of the simulations. The protein is represented as gray ribbons. The lipid phosphate headgroups are shown as a pale brown surface. A blue section of the protein indicates the anchor region (residues 708–730), which shows significantly reduced H/D exchange when the enzyme is in the membrane. The active site Ser519 is shown in CPK representation. A yellow volume indicates a cavity at the entrance of the active-site, which may be employed for the lipid extraction. The inserted side chains of three anchoring residues, Pro714, Trp715, and Leu717, are shown in CPK representations in brown, gray, and pink. (B) Close-up caption of the cluster of hydrophobic residues (Pro711, Pro714, Trp715, Leu717, Val721, Phe722) that are interacting with the lipid membrane. A horizontal line was drawn to indicate the approximate position of phosphate groups. The protein side chains are colored according to their charges (green = polar; gray = hydrophobic; blue = positively charged; red = negatively charged). (C) Equilibration of hydrogen bond interactions between the protein and the lipid headgroups during a 60 ns AA-MD simulation. (D) Time series of the insertion angle in three 60 ns AA-MD simulations.
doi:10.1371/journal.pcbi.1003156.g003

along the bilayer normal (*z* axis). In both CG-MD and AA-MD simulations, a similar distribution of residues was observed with respect to the components of the bilayer system (Figure 4A). Among the different surface residues, the positions of basic (Arg710, and Lys719) and polar residues (Ser712, Asn713, Glu716, Thr720, and Gly723) were found to coincide roughly with the phosphate peak, at ~ 18.9 (± 1.6) Å from the bilayers center (Table 1). The cluster of hydrophobic residues (Pro711, Pro714, Trp715, Leu717, Val721, and Phe722) was found to be

inserted ~ 3 Å deeper into the membrane in a region occupied by the lipid tails. The perturbation induced by the anchor residues on the vertical packing of the lipids was found to be small. In all six simulations, the location of the catalytic site residue Ser519 was at least 10 Å away from the lipid headgroups, and at an average distance of ~ 36 Å from the membrane center. This strongly suggests that the phospholipid substrate molecule must be extracted from the membrane at the beginning of the catalytic reaction.

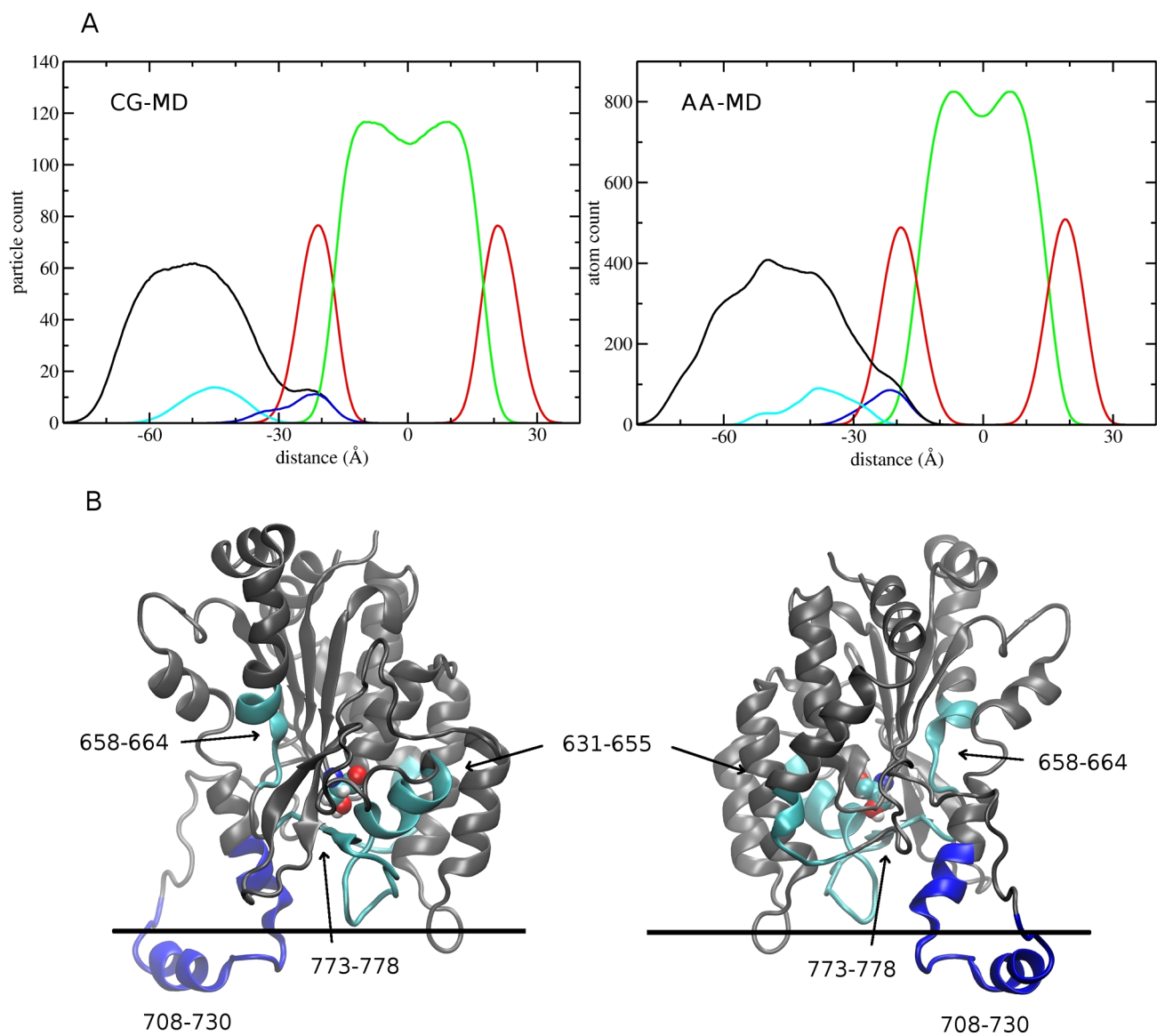


Figure 4. (A) Distribution of residues with respect to the components of the bilayer system (lipid headgroups and tails; red and green, respectively). The protein (black) was magnified $\times 3$ times for better visualization. Also shown is the distribution of hydrophobic anchors (blue) and surface residues (ice-blue) that only showed a small decrement in H/D exchange when in contact with the membrane. (B) DXMS results are color-mapped on the protein model: gray residues did not show a decrement in H/D exchange when the protein was in the membrane, blue residues showed a $>70\%$ decrement after 5 min of incubation time, while ice-blue corresponds to a smaller $<40\%$ effect after 5 min. The approximate position of the phosphate peak is shown as a horizontal line. The active site Ser591 is drawn in a CPK representation. doi:10.1371/journal.pcbi.1003156.g004

Comparison between equilibrated structures and DXMS experiments

DXMS experiments were carried out on the Group VIA-2 iPLA₂ enzyme, which is composed of seven consecutive N-terminal ankyrin repeats, a linker region, and a C-terminal phospholipase catalytic domain. Deuterium exchange on iPLA₂ was carried out in the presence of the phospholipid substrate, palmitoyl-arachidonyl-phosphatidylcholine (PAPC), and a methyl arachidonyl fluorophosphonate (MAFP) inhibitor to prevent the digestion of the membrane. It identified four regions with significant changes in deuterium exchange upon membrane binding, all located in the catalytic domain (Figure 4B). The region 708–730 showed the largest deuteration levels ($>90\%$) in solution, showing that it is solvent-exposed in the absence of

phospholipid vesicles. However, in the presence of phospholipid vesicles, the same region did not become highly deuterated, suggesting that it is involved in the membrane anchoring and therefore no longer solvent accessible. When the incubation time in D₂O was 10 s, mass spectrometry shows a difference of 13.2 in the average number of deuterium exchanges for this region. Similarly, in the case of a 5 min incubation time, a $\sim 70\%$ decrease in deuteration levels was measured in the presence of the membrane. The computational models are consistent with this result, as they show that hydrophobic residues Val708, Phe709, Trp715, Leu717, Val721, Phe722, and Leu727, are no longer solvent-accessible in the protein-membrane complex. Interestingly, the negatively charged region 773–778 and the regions 631–655 and 658–664 also showed a decrease of deuteration that is

Table 1. Location of surface side-chains relative to the bilayer center.

Residue type	Residue	AA-MD
hydrophobic	Pro711	16.8±1.9
	Pro714	16.4±2.0
	Trp715	15.0±1.7
	Leu717	19.0±2.2
	Val721	15.2±1.6
	Phe722	13.7±1.6
		16.0±1.8
basic	Arg710	19.0±2.2
	Lys719	18.3±1.6
		18.6±1.9
polar	Ser712	19.4±1.8
	Asn713	20.6±2.0
	Glu716	20.7±1.7
	Thr720	17.2±2.0
	Gly723	18.9±1.6
		19.3±1.8

Average ± standard deviation (Å) of the distance between the center of mass of the residue and the center of mass of the bilayer. Averages were taken over the last 20 ns of six AA-MD simulations.

doi:10.1371/journal.pcbi.1003156.t001

however less pronounced than for the anchor residues (<40% decrease in deuteration levels after 5 min of incubation). In the computational models, these residues belong to a hydrophobic cavity at the membrane surface that leads to the active-site serine. A likely explanation for the weak observed DMXS effect is that a single phospholipid can transiently occupy the cavity, and prevent the solvent from accessing these residues. We are currently exploring this hypothesis in more details and will publish these results separately.

AA-MD simulations of iPLA₂ in solution

In order to detect properties of the enzyme that change upon binding to the membrane, we compared two simulations of iPLA₂, in solution, and in a membrane. In both these simulations, the RMSD for the protein backbone atoms was found to stabilize below 3 Å, which is indicative of a stable protein model (Figure 5A). Moreover, both simulations showed that the anchor region of iPLA₂ (710–724) is very dynamic in nature (Figure 5B). However, in solution the amphipathic helix was observed to unfold, indicating that it is stabilized by the interaction with the membrane [42]. In addition, residues of the anchor region were found to move in solution by as much as ~7 Å, and in some structures to block the entrance of the active-site cavity (Figure 5C). In particular, the bulky Tyr643 residue was found to act as a gatekeeper that can prevent the entrance of incoming ligands. To show this, the free energy profile was calculated for a methane probe entering the active-site with the implicit ligand sampling (ILS) method [43]. The ILS method allows the rapid post-processing an entire MD trajectory to collect qualitative information about the interaction free energy of a small probe. The calculation showed that a favorable free energy pathway exists connecting the membrane to the catalytic Ser519, which is accessible only in the membrane-activated (open) state of the protein (Figure 5D). This uncovers a new mechanism by which the

flexible anchor region of iPLA₂ may provide a form of active-site regulation similar to the lid structure in cPLA₂.

Discussion

The present study on iPLA₂ complements two previous CG simulation studies [10,44] that also demonstrated the utility of a multi-resolution simulation approach for predicting the surface location of PLA₂ enzymes. These two previously published CG studies focused on the smaller sPLA₂ (~14–19 kDa), which has a known structure, and bears no sequence similarity with the much larger iPLA₂ (~84–90 kDa). In one study [10], it was found that the sPLA₂ protein equilibrated further away from the membrane than suggested by experiments. However, the authors concluded that these differences were most likely due to difficulties in interpreting tryptophan fluorescence experiments, as no drift was observed in their AA-MD simulations originated from the CG models. In support for this explanation, no drift was observed here in the AA-MD simulations originated from the CG models, and the agreement between computer simulations and DXMS experiments was excellent for the prediction of membrane-bound residues.

Our results show that the catalytic domain of iPLA₂ adopts a well-defined orientation at the membrane surface that is aimed to facilitate the vertical extraction of phospholipids from the membrane. Both the insertion depth and the orientation of iPLA₂ on the lipid surface are therefore finely tuned to facilitate rapid turnover by coupling hydrolysis and product release with the binding of the next substrate [19,20]. In addition, the enzyme was observed to diffuse laterally at the membrane surface without any disruption of the membrane complex, with the lipids dynamically repacking around the enzyme. This lateral motion is in agreement with the so-called scooting mechanism, which has been proposed to be important to facilitate the detection of lipid protrusion at the membrane surface [45]. The scooting mechanism contrasts with the hopping mechanism, in which the enzyme dissociates and re-associates with the membrane to explore the lipid surface. The hopping mechanism is believed to be favored by sPLA₂ in the presence of zwitterionic membranes [44].

The Group VIA-2 splice variant of the iPLA₂ contains in addition to the catalytic domain, seven ankyrin repeats, and a linker region (~700 residues). The ankyrin repeats are believed to directly or indirectly assist membrane association because the catalytic domain by itself does not have activity [46]. Our efforts to simulate the full GVIA-2 iPLA₂ structure did not uncover an alternative mechanism for the membrane insertion in the presence of ankyrin repeats. In particular, two CG-MD simulations of the full GVIA-2 iPLA₂ structure were conducted for 500 ns starting from a random configuration of the lipids. After insertion into the membrane, no significant differences were observed in the catalytic domain region, suggesting that the catalytic domain *alone* is able to successfully complete the insertion process. However, it cannot be excluded that the additional structural elements increase the probability of membrane insertion, either by providing a second interaction point with the membrane, or by stabilizing the correct orientation of the catalytic domain. Moreover, the rotation of the catalytic domain around an axis perpendicular to the membrane plane was hindered in the full protein structure, which may be indicative of a more stable protein–membrane complex. Group VIA iPLA₂ has also been shown to be active as an oligomer through radiation inactivation studies [47]; thus, the ankyrin repeats may be crucial for stabilizing the complex by taking part in the assembly of an oligomeric structure.

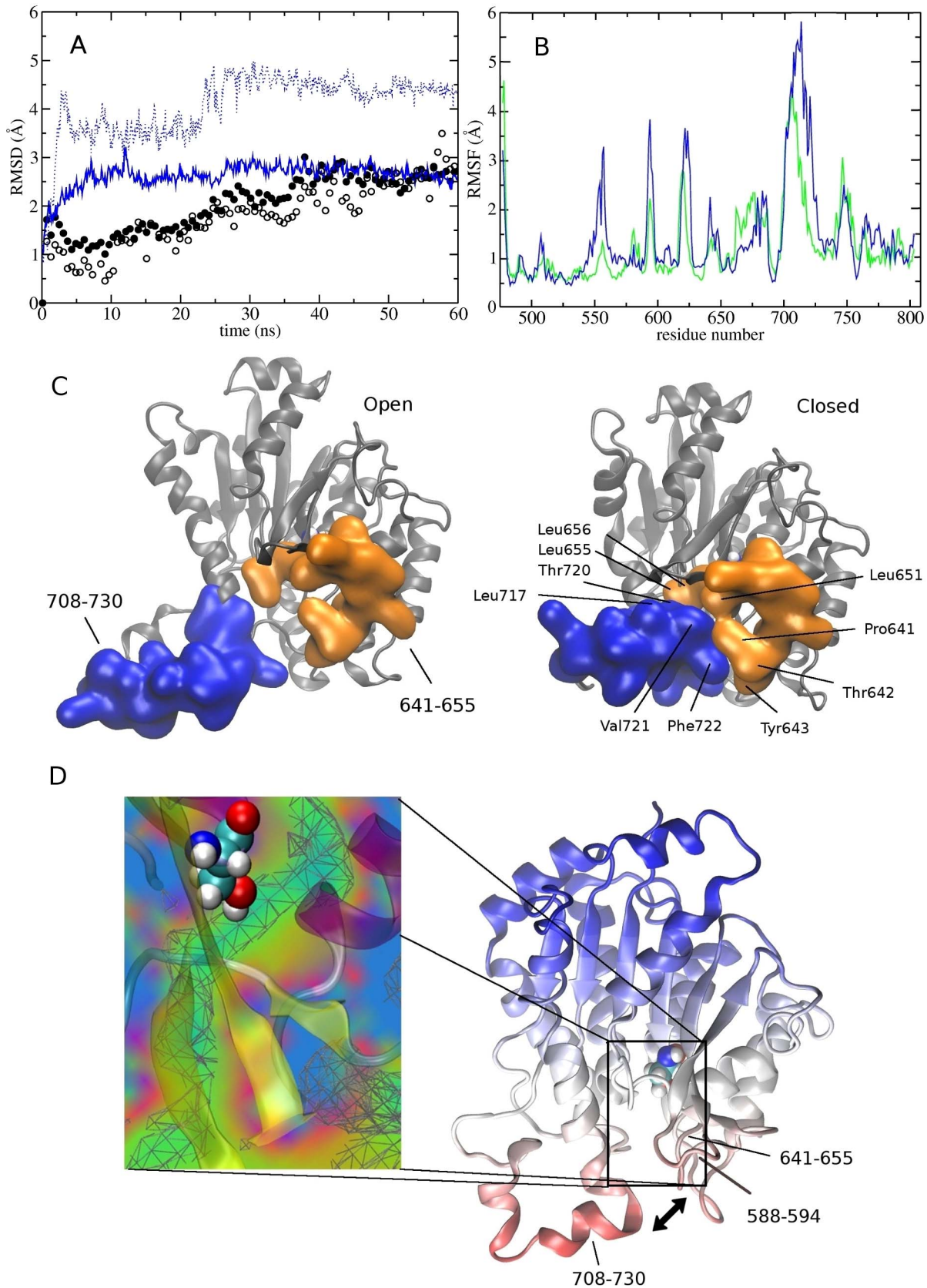


Figure 5. MD simulation of the iPLA₂ catalytic domain in solution and in the membrane. (A) Root-mean-square-deviations (RMSD) of backbone atoms for the protein (in the membrane, and in solution, full, and empty circles, respectively), and for anchoring residues 708–730 (in the membrane, and in solution, solid blue line, and dotted line, respectively). (B) Root-mean-square-fluctuations (RMSF) of different residues when the

protein is in the membrane (green) and in solution (blue). (C) In the absence of the membrane, the exposed hydrophobic residues of the anchor region are no longer stable in solution and can collapse, leading to a closed conformation of the entrance cavity. (D) Calculated free energy pathway for a hydrophobic (methane) probe entering the active-site cavity when the protein is in the open conformation. Green-blue regions correspond to a favorable (negative) free energy.
doi:10.1371/journal.pcbi.1003156.g005

For a successful hydrolysis of phospholipids, one substrate molecule must be extracted from the lipid aggregate into the active-site of iPLA₂. Because natural fluctuations in the fluid membrane mostly cause lateral motions in the lipid molecules, an exquisite mechanism must exist to allow the lipid molecule to escape the lipid surface. The structure of the iPLA₂-membrane complex shows the existence of a hydrophobic cavity near the membrane surface that is likely to assist the lipid extraction by competing with hydrophobic interactions between the substrate and the lipid aggregates. The deuterium exchange experiments also support a scenario in which the cavity is often transiently occupied by a lipid substrate extracted from the membrane. However, the lipid extraction could not be directly observed in our simulations, presumably because the lipid-binding cavity remained closed in the CG simulations due to the use of an elastic network model to stabilize the protein structure. In the AA simulations the time-scale (nanoseconds) was too short to observe the opening of the cavity and the extraction of a lipid from the membrane. Ongoing work in our labs will address this problem by conducting longer time-scale (microsecond) AA simulations, as well as steered MD simulations [48], and provide a more complete picture of the lipid extraction.

The high degree of conformational flexibility of iPLA₂ during simulations leads us to believe that the flexible loops that form the entrance of the cavity regulate the active-site accessibility. For instance, the hydrophobic residues in the anchor region (710 to 724) fold into an amphipathic helix in the membrane, but adopt an extended conformation when they are in solution, leading to the partial closure of the active-site cavity. We [27] have recently hypothesized that each type of PLA₂ contains a distinct “membrane interaction site(s)” that should be considered as a typical allosteric site. When the PLA₂ is associated with a ligand (in this case, the membrane), the enzyme exists in a different conformational state than in solution (R to T transition) in accord with the basic ideas of allostery [49] as recently reviewed by Changeux [50]. Although further work will be needed to confidently map the conformational landscape of iPLA₂, the results reported herein are consistent with the novel notion of

considering the membrane as a ligand, which causes a conformational change in certain water-soluble proteins (such as various PLA₂s) when they productively associate with a membrane [27]. In addition, the present study identified an amphipathic helix as the anchor region of iPLA₂. Amphipathic helices have been recently proposed as interesting motifs that help recognize hydrophobic defects in the membrane, such as those created when bending the bilayer [42,51,52]. It is possible that the helix in iPLA₂ confers the enzyme with the ability to detect membrane defects, which is believed to be a key property of PLA₂s [45].

In future studies, a deeper understanding should be gained of the roles of different protein conformations accessed during the catalytic cycle of iPLA₂. This will be crucial for inhibitor design, as interrupting a single catalytic step could be sufficient to inhibit the entire reaction. MD simulations could be utilized to explore the role of the enzyme flexibility during the different phases of the catalytic process, including the extraction, binding, and hydrolysis of the substrate and the release of the products in the bilayer. These models will open the door to virtual screening techniques aimed at finding new inhibitors of iPLA₂ with improved potency and selectivity. Finally, we feel that the multi-scale approach discussed here should prove helpful in designing initial computational models of various PLA₂ enzymes at the membrane surface, and will lead to further studies on the impact of lipid diversity and sequence mutations on the activity of iPLA₂ and related enzymes.

Supporting Information

Text S1 Atomic coordinates of the protein-membrane system after AA-MD refinement, in the protein database (PDB) format. (DOC)

Author Contributions

Conceived and designed the experiments: DB YHH VDM EAD JAM. Performed the experiments: DB YHH. Analyzed the data: DB YHH. Contributed reagents/materials/analysis tools: DB YHH VDM EAD JAM. Wrote the paper: DB YHH VDM EAD JAM.

References

- Dennis EA, Cao J, Hsu YH, Magrioti V, Kokotos G (2011) Phospholipase A2 enzymes: physical structure, biological function, disease implication, chemical inhibition, and therapeutic intervention. *Chem Rev* 111: 6130–6185.
- Lacapere JJ, Pebay-Peyroula E, Neumann JM, Etchebest C (2007) Determining membrane protein structures: still a challenge! *Trends in Biochemical Sciences* 32: 259–270.
- MacCallum JL, Perez A, Schnieders MJ, Hua L, Jacobson MP, et al. (2011) Assessment of protein structure refinement in CASP9. *Proteins-Structure Function and Bioinformatics* 79: 74–90.
- Raval A, Piana S, Eastwood MP, Dror RO, Shaw DE (2012) Refinement of protein structure homology models via long, all-atom molecular dynamics simulations. *Proteins-Structure Function and Bioinformatics* 80: 2071–2079.
- Tozzini V (2005) Coarse-grained models for proteins. *Current Opinion in Structural Biology* 15: 144–150.
- Marrink SJ, Risselada HJ, Yefimov S, Tieleman DP, de Vries AH (2007) The MARTINI force field: Coarse grained model for biomolecular simulations. *Journal of Physical Chemistry B* 111: 7812–7824.
- Monticelli L, Kandasamy SK, Periole X, Larson RG, Tieleman DP, et al. (2008) The MARTINI coarse-grained force field: Extension to proteins. *Journal of Chemical Theory and Computation* 4: 819–834.
- Bond PJ, Sansom MSP (2006) Insertion and assembly of membrane proteins via simulation. *Journal of the American Chemical Society* 128: 2697–2704.
- Thogersen L, Schiott B, Vosegaard T, Nielsen NC, Tajkhorshid E (2008) Peptide Aggregation and Pore Formation in a Lipid Bilayer: A Combined Coarse-Grained and All Atom Molecular Dynamics Study. *Biophysical Journal* 95: 4337–4347.
- Wee CL, Balali-Mood K, Gavaghan D, Sansom MSP (2008) The interaction of phospholipase A2 with a phospholipid bilayer: Coarse-grained molecular dynamics simulations. *Biophysical Journal* 95: 1649–1657.
- Balali-Mood K, Bond PJ, Sansom MSP (2009) Interaction of Monotopic Membrane Enzymes with a Lipid Bilayer: A Coarse-Grained MD Simulation Study. *Biochemistry* 48: 2135–2145.
- Ayton GS, Noid WG, Voth GA (2007) Multiscale modeling of biomolecular systems: in serial and in parallel. *Current Opinion in Structural Biology* 17: 192–198.
- Lyman E, Ytreberg FM, Zuckerman DM (2006) Resolution exchange simulation. *Physical Review Letters* 96: 028105.
- Mouchlis VD, Barbayanni E, Mavromoustakos TM, Kokotos G (2011) The Application of Rational Design on Phospholipase A(2) Inhibitors. *Current Medicinal Chemistry* 18: 2566–2582.
- Buczynski MW, Dumlao DS, Dennis EA (2009) Thematic Review Series: Proteomics. An integrated omics analysis of eicosanoid biology. *J Lipid Res* 50: 1015–1038.
- Cao J, Burke JE, Dennis EA (2013) Using Hydrogen-Deuterium Exchange Mass Spectrometry to Define the Specific Interactions of the Phospholipase A2

- Superfamily with Lipid Substrates, Inhibitors and Membranes. *J Biol Chem* 288: 1806–1813.
17. Winget JM, Pan YH, Bahnson BJ (2006) The interfacial binding surface of phospholipase A₂s. *Biochim Biophys Acta* 1761: 1260–1269.
 18. Gijon MA, Spencer DM, Kaiser AL, Leslie CC (1999) Role of phosphorylation sites and the C2 domain in regulation of cytosolic phospholipase A₂. *J Cell Biol* 145: 1219–1232.
 19. Cao J, Hsu YH, Li S, Woods VL, Dennis EA (2011) Lipoprotein-associated phospholipase A(2) interacts with phospholipid vesicles via a surface-disposed hydrophobic alpha-helix. *Biochemistry* 50: 5314–5321.
 20. Hsu YH, Burke JE, Li S, Woods VL, Jr., Dennis EA (2009) Localizing the membrane binding region of Group VIA Ca²⁺-independent phospholipase A₂ using peptide amide hydrogen/deuterium exchange mass spectrometry. *J Biol Chem* 284: 23652–23661.
 21. Talbot K, Young RA, Jolly-Tornetta C, Lee VMY, Trojanowski JQ, et al. (2000) A frontal variant of Alzheimer's disease exhibits decreased calcium-independent phospholipase A₂ activity in the prefrontal cortex. *Neurochemistry International* 37: 17–31.
 22. Zachman DK, Chicco AJ, McCune SA, Murphy RC, Moore RL, et al. The role of calcium-independent phospholipase A₂ in cardiomyocyte remodeling in the spontaneously hypertensive heart failure rat heart. *J Lipid Res* 51: 525–534.
 23. Gregory A, Westaway SK, Holm IE, Kotzbauer PT, Hogarth P, et al. (2008) Neurodegeneration associated with genetic defects in phospholipase A(2). *Neurology* 71: 1402–1409.
 24. Kalyvas A, Baskakis C, Magrioti V, Constantinou-Kokotou V, Stephens D, et al. (2009) Differing roles for members of the phospholipase A(2) superfamily in experimental autoimmune encephalomyelitis. *Brain* 132: 1221–1235.
 25. Scott KF, Sajinovic M, Hein J, Nixdorf S, Galetti P, et al. (2010) Emerging roles for phospholipase A(2) enzymes in cancer. *Biochimie* 92: 601–610.
 26. Kokotos G, Hsu YH, Burke JE, Baskakis C, Kokotos CG, et al. (2010) Potent and Selective Fluoroketone Inhibitors of Group VIA Calcium-Independent Phospholipase A(2). *Journal of Medicinal Chemistry* 53: 3602–3610.
 27. Burke JE, Babakhani A, Gorf AA, Kokotos G, Li S, et al. (2009) Location of Inhibitors Bound to Group IVA Phospholipase A(2) Determined by Molecular Dynamics and Deuterium Exchange Mass Spectrometry. *Journal of the American Chemical Society* 131: 8083–8091.
 28. Hsu Y, Bucher D, Cao J, Yang S, Kokotos G, et al. (2013) Fluoroketone inhibition of Ca²⁺-independent phospholipase A₂ through binding pocket association observed by hydrogen/deuterium exchange and molecular dynamics. *J Amer Chem Soc* 135: 1330–1337.
 29. Rydel TJ, Williams JM, Krieger E, Moshiri F, Stallings WC, et al. (2003) The crystal structure, mutagenesis, and activity studies reveal that patatin is a lipid acyl hydrolase with a Ser-Asp catalytic dyad. *Biochemistry* 42: 6696–6708.
 30. Jacobson MP, Pincus DL, Rapp CS, Day TJJ, Honig B, et al. (2004) A hierarchical approach to all-atom protein loop prediction. *Proteins-Structure Function and Bioinformatics* 55: 351–367.
 31. Hess B, Kutzner C, van der Spoel D, Lindahl E (2008) GROMACS 4: Algorithms for highly efficient, load-balanced, and scalable molecular simulation. *Journal of Chemical Theory and Computation* 4: 435–447.
 32. Periole X, Cavalli M, Marrink SJ, Ceruso MA (2009) Combining an Elastic Network With a Coarse-Grained Molecular Force Field: Structure, Dynamics, and Intermolecular Recognition. *Journal of Chemical Theory and Computation* 5: 2531–2543.
 33. Yang HC, Mosior M, Ni BH, Dennis EA (1999) Regional distribution, ontogeny, purification, and characterization of the Ca²⁺-independent phospholipase A(2) from rat brain. *Journal of Neurochemistry* 73: 1278–1287.
 34. Bussi G, Donadio D, Parrinello M (2007) Canonical sampling through velocity rescaling. *Journal of Chemical Physics* 126: 014101.
 35. Berendsen HJC, Postma JPM, Vangunsteren WF, Dinola A, Haak JR (1984) Molecular-Dynamics with Coupling to an External Bath. *Journal of Chemical Physics* 81: 3684–3690.
 36. Humphrey W, Dalke A, Schulten K (1996) VMD: Visual molecular dynamics. *Journal of Molecular Graphics & Modelling* 14: 33–38.
 37. Phillips JC, Braun R, Wang W, Gumbart J, Tajkhorshid E, et al. (2005) Scalable molecular dynamics with NAMD. *Journal of Computational Chemistry* 26: 1781–1802.
 38. Best RB, Zhu X, Shim J, Lopes PEM, Mittal J, et al. (2012) Optimization of the Additive CHARMM All-Atom Protein Force Field Targeting Improved Sampling of the Backbone phi, psi and Side-Chain chi(1) and chi(2) Dihedral Angles. *Journal of Chemical Theory and Computation* 8: 3257–3273.
 39. Klauda JB, Venable RM, Freites JA, O'Connor JW, Tobias DJ, et al. (2010) Update of the CHARMM All-Atom Additive Force Field for Lipids: Validation on Six Lipid Types. *Journal of Physical Chemistry B* 114: 7830–7843.
 40. Ryckaert JP, Ciccotti G, Berendsen HJC (1997) Numerical-Integration of Cartesian Equations of Motion of a System with Constraints - Molecular-Dynamics of N-Alkanes. *Journal of Computational Physics* 23: 327–341.
 41. Adelman SA, Doll JD (1976) Generalized Langevin Equation Approach for Atom-Solid-Surface Scattering - General Formulation for Classical Scattering Off Harmonic Solids. *Journal of Chemical Physics* 64: 2375–2388.
 42. Cui HS, Lyman E, Voth GA (2011) Mechanism of Membrane Curvature Sensing by Amphipathic Helix Containing Proteins. *Biophysical Journal* 100: 1271–1279.
 43. Cohen J, Olsen KW, Schulten K (2008) Finding gas migration pathways in proteins using implicit ligand sampling. *Globins and Other Nitric Oxide-Reactive Proteins, Part B* 437: 439–457.
 44. Qin SS, Yu YX, Li QK, Yu ZW (2013) Interaction of Human Synovial Phospholipase A2 with Mixed Lipid Bilayers: A Coarse-Grain and All-Atom Molecular Dynamics Simulation Study. *Biochemistry* 52: 1477–1489.
 45. Hoyrup P, Callisen TH, Jensen MO, Halperin A, Mouritsen OG (2004) Lipid protrusions, membrane softness, and enzymatic activity. *Physical Chemistry Chemical Physics* 6: 1608–1615.
 46. Larsson PKA, Claesson HE, Kennedy BP (1998) Multiple splice variants of the human calcium-independent phospholipase A(2) and their effect on enzyme activity. *Journal of Biological Chemistry* 273: 207–214.
 47. Balboa MA, Balsinde J, Jones SS, Dennis EA (1997) Identity between the Ca²⁺-independent phospholipase A(2) enzymes from P388D(1) macrophages and Chinese hamster ovary cells. *Journal of Biological Chemistry* 272: 8576–8580.
 48. Stepaniants S, Izrailev S, Schulten K (1997) Extraction of lipids from phospholipid membranes by steered molecular dynamics. *Journal of Molecular Modeling* 3: 473–475.
 49. Monod J, Wyman J, Changeux JP (1965) On Nature of Allosteric Transitions - a Plausible Model. *Journal of Molecular Biology* 12: 88–&.
 50. Changeux JP (2012) Allostery and the Monod-Wyman-Changeux Model After 50 Years. *Annual Review of Biophysics* 41: 103–133.
 51. Hatzakis NS, Bhatia VK, Larsen J, Madsen KL, Bolinger PY, et al. (2009) How curved membranes recruit amphipathic helices and protein anchoring motifs. *Nature Chemical Biology* 5: 835–841.
 52. Vanni S, Vamparys L, Gautier R, Drin G, Etchebest C, et al. (2013) Amphipathic Lipid Packing Sensor Motifs: Probing Bilayer Defects with Hydrophobic Residues. *Biophysical Journal* 104: 575–584.